Optical properties of chromium(III) in $M^{I}In(MoO_4)_2$ hosts, where M^{I} = Li, Na, K, Rb, Cs

2001 J. Phys.: Condens. Matter 13 5807

(http://iopscience.iop.org/0953-8984/13/25/307)

INSTITUTE OF PHYSICS PUBLISHING JOURNAL OF PHYSICS: CONDENSED MATTER

J. Phys.: Condens. Matter **13** (2001) 5807–5816 www.iop.org/Journals/cm PII: S0953-8984(01)16121-7

Optical properties of chromium(III) in $M^{I}In(MoO_4)_2$ hosts, where M^{I} = Li, Na, K, Rb, Cs

K Hermanowicz[1], J Hanuza[1], M Mączka[1], P J Dereń[1], E Mugeński[1], H Drulis[1], I Sokolska[1] and J Sokolnicki[2]

[1] Institute for Low Temperature and Structure Research, Polish Academy of Sciences, PO Box 1410, 50-950 Wroclaw 2, Poland
[2] Faculty of Chemistry, University of Wroclaw, Wroclaw, Poland

Received 7 August 2000, in final form 14 March 2001

Abstract

Electron absorption, excitation and emission as well as electron spin-resonance spectra were measured for orthorhombic (K, Rb, Cs) and monoclinic (Li, Na) $M^{I}Cr_xIn_{1-x}(MoO_4)_2$ ($x = 0.5$–2%, M^{I} = Li, Na, K, Rb, Cs) in the temperature range 5–300 K. The local structure of the Cr^{3+} ions is discussed on the basis of spectroscopic results and the crystal-field parameters are derived for all of the materials. The possible application of the compounds studied as laser materials is discussed.

1. Introduction

Double molybdates of the $M^{I}M^{III}(MoO_4)_2$ family are very important compounds because of their optical, antiferroelectric and ferroelastic properties [1–9]. They are suitable hosts for transition-metal and lanthanide ions [10–12]. The aim of the present studies is characterization of spectroscopic properties of these new materials, which are prospective laser media. As far as we are aware, the spectroscopic properties of the alkali metal–indium double molybdates have not been studied yet.

2. Experiment

Double molybdates were grown by the thermal method developed by Klevtsov *et al* [13] with the cooling rate 2 K per hour. The mixtures of the chemically pure materials $M^{I}_2CO_3$ (M^{I} = Li, Na, K, Rb, Cs), In_2O_3 and MoO_3 were prepared so as to obtain a 1:1 ratio between the $M^{I}In(MoO_4)_2$ double molybdate and the solvent ($M^{I}_2Mo_2O_7$). The crystals obtained were of good optical quality. The lattice parameters for the single crystals, measured using an x-ray diffractometer, were in good agreement with the literature data [14–16].

The absorption spectra were measured using Cary SE spectrophotometer. The resolution was 5 cm^{-1}.

0953-8984/01/255807+10$30.00

The emission spectra were recorded with a THR 1000 Jobin-Yvon monochromator. A highly sensitive photomultiplier, R928 Hamamatsu, was used for detection of the spin-forbidden transition as well as the decay profiles. A PbS-cooled detector was used to detect the spectra in the NIR region.

A SR400 Stanford photon-counting system was used for the measurements of the decay profiles. The excitation sources were an excimer laser from Lambda Physik Company, and a krypton ILK120 laser from Carl Zeiss (Jena).

ESR spectra for the polycrystalline state were measured in the 5–300 K temperature range with an X-band Radiopan Spectrometer. The magnetic field was calibrated with a nuclear MJ110R magnetometer.

3. Results and discussion

3.1. Crystal structure of the hosts

$M^{I}In(MoO_4)_2$ crystals are attractive hosts for doping with Cr^{3+} ions. An especially important feature of these crystals is the fact that they are not isostructural, although their structures are derived from the structure of scheelite (for Na, K, Rb and Cs) or wolframite (for Li). This allows us to compare the spectroscopic properties of the Cr^{3+} ion in different environments.

The low-temperature modification of $LiIn(MoO_4)_2$ is monoclinic $C2/c = C_{2h}^6$ with $Z = 4$. The unit-cell dimensions are: $a = 9.504$ Å, $b = 11.459$ Å, $c = 4.994$ Å and $\beta = 91.49^\circ$ [17]. The crystal is built up of MoO_4^{2-} ions connected to each other by means of intermolecular interactions of the $W^{O}{}_{O}W$ type, forming chains along the c-direction. The two different W–O distances are 2.36 and 2.07 Å, and therefore the oxygen bridge symmetry is C_1. The molybdenum(VI) ions are octahedrally coordinated to oxygen atoms occupying the sites of C_1 symmetry. This type of structure is characterized by the following coordination numbers (CN) and site symmetries (SS):

$$\begin{array}{lll} CN(Li^+) = 6 & CN(In^{3+}) = 6 & CN(Mo^{6+}) = 6 \\ SS(Li^+) = C_2 & SS(In^{3+}) = C_2 & SS(Mo^{6+}) = C_1. \end{array}$$

In the chromium-doped crystal the activator replaces the In^{3+} ions, occupying the C_2 site symmetry. The In–O distances in this polyhedron are 2×2.0903 Å, 2×2.1455 Å and 2×2.2635 Å and the shortest In–In distance is 3.2794 Å.

$NaIn(MoO_4)_2$ crystallizes in the triclinic space group $P1 = C_i^1$ ($Z = 4$) with the lattice parameters $a = 7.18$ Å, $b = 7.18$ Å, $c = 14.90$ Å, $\alpha = 92^\circ$, $\beta = 88^\circ$ and $\gamma = 82^\circ$ [14]. In the paper [18] different parameters are given: $a = 14.77$ Å, $b = 7.15$ Å, $c = 7.15$ Å, $\alpha = 98.5^\circ$, $\beta = 92^\circ$ and $\gamma = 92$, although the space group is the same. In this crystal the MoO_4^{2-} tetrahedra occupy four and the cations two crystallographically non-equivalent sites of C_i symmetry. The chromium(III) ions replace cationic sites of C_i symmetry. Two In^{3+} ions are sixfold coordinated to the oxygen atoms, with In_1–O distances ranging from 2.14 to 2.24 Å and In_2–O ones from 2.06 to 2.27 Å. The In–In distance is larger than 5 Å.

Potassium–indium, rubidium–indium and caesium–indium double molybdates are isostructural. The low-temperature structure of these molybdates is orthorhombic, with the space group $Pnam = D_{2h}^{16}$ and four molecules in the unit cell [15, 16]. In this structure all cations are crystallographically equivalent and occupy sites of C_s symmetry. The MoO_4^{2-} ions form two sets of non-equivalent sites of C_s symmetry. The six indium–oxygen distances range from 2.1 to 2.23 Å and the In–In distance is larger than 5 Å. The chromium(III) ions in these crystals are doped into the cationic sites of C_s symmetry.

3.2. Absorption measurements

From the structural consideration it follows that two types of crystal have been studied: potassium, caesium and rubidium derivatives are orthorhombic and the Cr^{3+} ions occupy the single crystallographic site of C_s symmetry; the sodium crystal is triclinic and Cr^{3+} ions are located at two non-equivalent sites of C_i symmetry.

The absorption spectra of $MIn(MoO_4)_2$ (M = Na, K) were measured at low and room temperature (see figure 1). They are always composed of three broad bands (with halfwidth $\approx$ 120 nm) which are due to the spin-allowed transitions: $^4A_2 \rightarrow {}^4T_2$ ($\lambda_{max} \approx 740.4$ nm and $\lambda_{max} \approx 721.2$ nm for $NaIn(MoO_4)_2$ and $KIn(MoO_4)_2$ crystal, respectively), $^4A_2 \rightarrow {}^4T_1(F)$ ($\lambda_{max} \approx 500$ nm and $\lambda_{max} \approx 493.5$ nm, respectively) and $^4A_2 \rightarrow {}^4T_1(P)$ ($\lambda_{max} \approx 368$ nm and $\lambda_{max} \approx 370$ nm, respectively). The splitting due to the low symmetry and spin–orbit coupling of the quartet levels becomes apparent from the asymmetric shape of the bands and the presence of pronounced shoulders (see for example the $^4A_2 \rightarrow {}^4T_1(F)$ band). However, the splitting of the $^4A_2 \rightarrow {}^4T_2$ band suggests the presence of three peaks which cannot result from the overlap of two displaced Gaussian bands. Therefore, the dips should be considered, instead of maxima, which represent a reduction of absorption and were described as Fano antiresonances [17, 18] by several authors [19, 20].

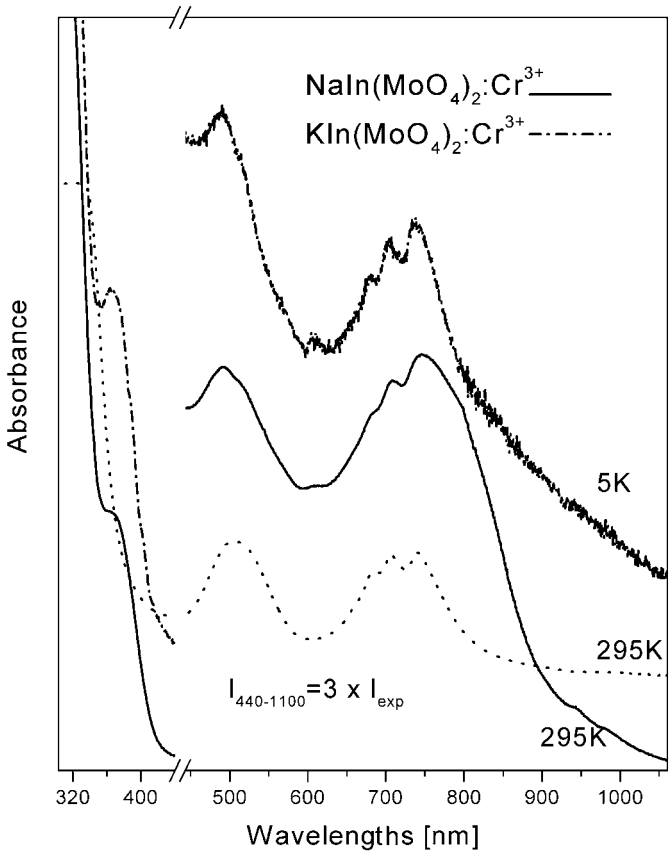

Figure 1. The absorption spectra of the Cr^{3+} ion observed at 295 K in the $NaIn(MoO_4)_2$ host and at 5 and 295 K in the $KIn(MoO_4)_2$ host.

The spin-forbidden transitions to the excited doublet levels can rarely be observed in the absorption spectra of Cr^{3+} ions. However, in some cases an interaction between the sharp intraconfigurational $t_2{}^3e$ levels (^2E and $^2T_1$) and the vibronically broadened $^4T_2$ ($t_2{}^2e$) quasicontinuum results in Fano-type antiresonance. Lempicki *et al* noted that the R lines do not coincide with the low-energy 'peak' [20]. This difference is due to coupling of the ^2E level with the continuum and the displacement is analogous to the Lamb shift [17]. Here it could be a consequence of broadening due to the presence of several Cr^{3+} sites and the lack of dependence of the ^2E level on the ligand field.

Indeed, in our previous work on $MCr(MoO_4)_2$ (M = Li, Na, K, Cs) [21] and on $MAl(MoO_4)_2{:}Cr^{3+}$ (M = Li, Na, K, Cs) crystals [22] we observed the position of the ^2E level at about 13 500 cm^{-1} and there is no reason to suppose that in other scheelite crystals the position of the ligand-field-independent level will change drastically. Therefore, we read the position of the ^2E level on the lower-energy side of the dip, in a similar way to in [20]. The energy values of the Cr^{3+} levels are shown in table 1, together with the crystal-field and Racah parameters. The low value of the Dq/B ratio, where $Dq/B = 2.3$ shows that the field is intermediate, indicates that the Cr^{3+} ions are in a low ligand field with the minimum of the $^4T_2$ level lying below the minimum of the doublet level. Therefore, one anticipates that broad-band emission and relatively fast decay will be observed.

Table 1. Energy levels, crystal-field and Racah parameters, the Stokes shift E_m, the Huang–Rhys parameter S and ΔE (see the text for an explanation) obtained from the absorption and emission spectra of $MIn(MoO_4)_2{:}Cr^{3+}$ crystals, where M = K or Na.

	$KIn(MoO_4)_2$	$NaIn(MoO_4)_2$
$^4T_2$ (cm^{-1})	13860	13506
^2E (cm^{-1})	13630	13740
$^2T_1$ (cm^{-1})	14380	14240
$^4T_1$(F) (cm^{-1})	19380	19218
	20260	20000
$^4T_1$(P) (cm^{-1})	27170	26450
B (cm^{-1})	681	705
Dq/B	2.03	1,91
C (cm^{-1})	2902	2859
C/B	4.26	4.05
E_m (cm^{-1})	2870	2880
S	5.6	5.6
ΔE (cm^{-1})	−1205	−1674

3.3. Emission

Figure 2 shows the emission spectra of $MIn(MoO_4)_2$ (M = Na, K) observed at low temperature. According to our predictions and unlike for the aluminium scheelites, the emission bands are broad because they are due to the spin-allowed $^4T_2 \rightarrow {}^4A_2$ transition. The position of the emission bands changes with temperature (table 2), indicating the presence of several Cr^{3+} sites. No evidence of the $^2E \rightarrow {}^4A_2$ spin-forbidden transition has been found—either at 10 K or at 300 K—in agreement with the assumption that the Cr^{3+} ions are in a low ligand field. The data obtained allowed us to calculate the Huang–Rhys parameter S defined by the

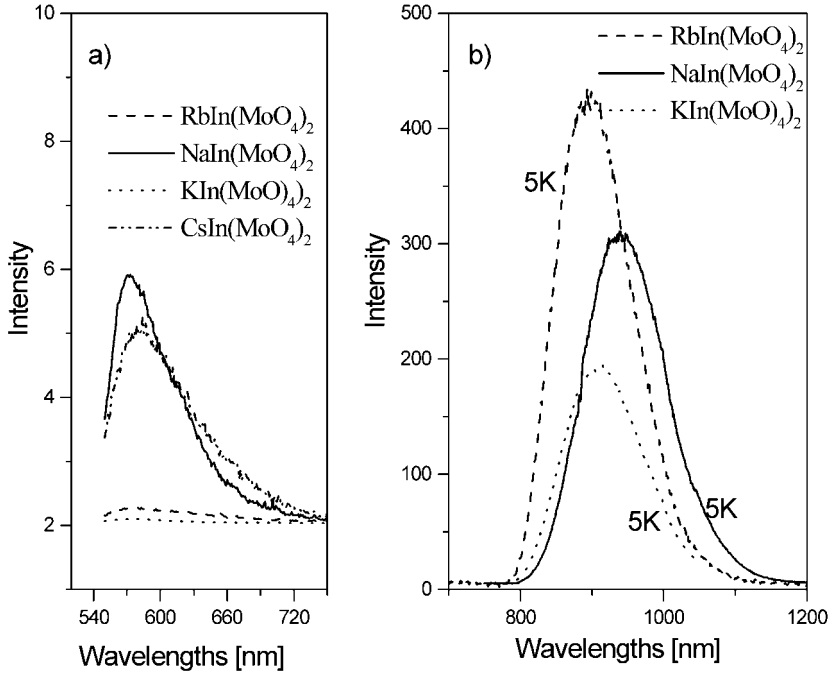

Figure 2. The emission measurements at 5 K for the hosts studied. For excitation, the 488 nm line of the argon laser was used.

Table 2. Maxima (in cm^{-1}) of the emission bands of $MIn(MoO_4)_2:Cr^{3+}$ crystals, where M = K, Rb, Cs and Na.

	$KIn(MoO_4)_2$	$RbIn(MoO_4)_2$	$CsIn(MoO_4)_2$	$KIn(MoO_4)_2$
5 K	10990	11150	—	10630
300 K	11220	10025	11075	10790

equation $E_m = (2S - 1)\hbar\omega$, where E_m and $\hbar\omega$ denote the Stokes shift and the energy of the effective phonons, respectively. For $\hbar\omega = 280$ cm^{-1} the high values of the S-parameter (see table 1) indicate strong electron–phonon coupling. The single-configurational model allows us also to calculate the difference ΔE between the minima of two $^4T_2$ and ^2E parabolas. The negative value of the ΔE parameter shows that the minimum of the $^4T_{2g}$ level is below the doublet level and that all excitation energy, after being stored in the metastable ^2E level, is transferred to the $^4T_{2g}$ level. As a result the broad emission is observed. The decay profiles of $KIn(MoO_4)_2:Cr^{3+}$ and $NaIn(MoO_4)_2:Cr^{3+}$ crystals are non-exponential, showing the presence of two Cr^{3+} sites (see figure 3), whereas the $RbIn(MoO_4)_2:Cr^{3+}$ crystal exhibits the decay of one Cr^{3+} site. The decay times of the fluorescence at 10 K are 71 and 140 μs for potassium, 69 and 167 μs for sodium and 146 μs for rubidium derivatives.

For the crystals investigated the shape of the broad emission bands was approximated with the equation $I_{em} = I_0 \sum \exp(-S)(S^m/m!)\delta(E_{00} - mh\nu - E)$, where S is the Huang–Rhys parameter, E_{00} is the zero-phonon energy, $h\nu$ is the effective phonon energy and m is an integer [23, 24]. In the first stage of the fitting procedure, the parameters S, $h\nu$ and E_{00} were roughly estimated from the spectroscopic data and the equations $SS = (2S-1)h\nu$, $H(0) = 2.36h\nu\sqrt{S}$ [24]. The former equation describes the Stokes shift (SS) between maxima of the absorption

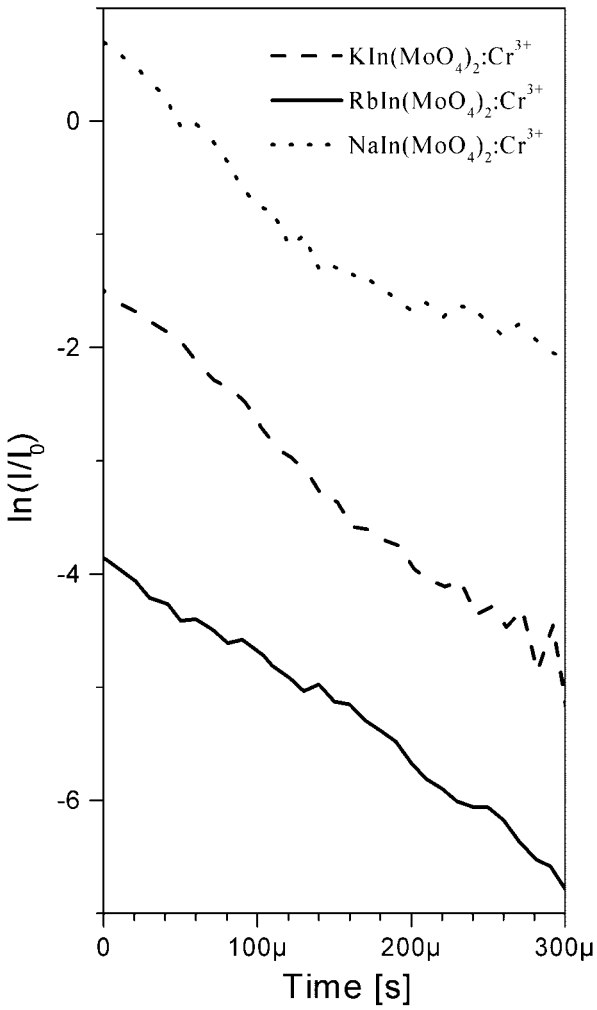

Figure 3. The emission decay curve for low-concentration samples (0.05–0.5 wt% of Cr^{3+}).

and emission bands and the latter the halfwidth H of the emission band at low temperature. The parameters obtained from the best fit of the low-temperature emission spectra to the predicted shape (figure 2) are given in table 3. For all the crystals the effective energy of the phonons involved is about 280 cm^{-1}. In this range, intense bands are observed in the IR and Raman spectra which correspond to the bending modes of molybdate ions [25–27].

Table 3. The parameters obtained from the fit of the predicted shape to the low-temperature emission spectra.

Crystal	E_{00} (cm^{-1})	$h\nu$ (cm^{-1})	S	$W_{nr}(0)$ (s^{-1})	λ_0 (nm)	$\Delta\lambda_{eff}$ (nm)	σ_{em}^{peak} (cm^2)
$NaIn(MoO_4)_2$	12180	270	5.95	1.24×10^{-10}	929	169	1.72×10^{-20}
$KIn(MoO_4)_2$	12480	287	5.47	1.38×10^{-10}	904	179	0.93×10^{-20}
$RbIn(MoO_4)_2$	12590	280	5.40	3.7×10^{-12}	899	182	0.75×10^{-20}

An important parameter describing materials for possible laser application is the emission cross section at room temperature, which can be calculated from the Füchtbauer–Ladenburg equation [28] $\sigma_{em}^{peak} = \lambda_0^4/(8\pi cn^2\tau_r\,\Delta\lambda_{eff})$, where λ_0 is the wavelength at the maximum emission, n is the refractive index of the material (approximately 2.05 for the crystals investigated), τ_r is the radiative lifetime (usually independent of the temperature) and $\Delta\lambda_{eff}$ is the effective width of the emission spectrum at room temperature defined as $\Delta\lambda_{eff} = \int I(\lambda)\,\mathrm{d}\lambda/I_0$. We have used in the calculations the low-temperature lifetime values as the radiative lifetimes. This assumption is justified by the low rate of non-radiative transitions at low temperature calculated according to the formula $W_{nr}(0) = R_{nr}(\mathrm{e}^{p-s}/\sqrt{2\pi p})(S/p)^p$, where R_{nf} is the non-radiative decay constant and lies in the range from 10^{12} to 10^{14} s^{-1} [29]. p is the number of phonons bridging the energy gap between the excited and ground states ($p = E_{00}/h\nu$) and S is the Huang–Rhys parameter. Values of the non-radiative transition rates at low temperature, the peak wavelengths λ_0 at RT, the effective widths $\Delta\lambda$ and the values of the emission cross sections finally obtained are summarized in table 3. The emission cross section values are of the typical order for Cr^{3+} materials.

The green emission observed for the crystals studied merits special attention. The intensity of this band does not depend on the chromium content. On the other hand, the intensity of the fluorescence at 800–900 nm significantly decreases in the sequence Rb, Na, K, Cs. In the extreme case, for the $CsIn(MoO_4)_2$ molybdate, the green emission at 574 nm is very much stronger than the red fluorescence of chromium (figure 2). Since the green emissions are similar for all the double molybdates studied, the differences in relative intensities of the two luminescence bands are due only to the changes in intensity of the red luminescence. The low intensity of the red luminescence in the case of $CsIn(MoO_4)_2$ can most probably be attributed to the poor quality of the crystals obtained: the crystals are opaque as a result of the high-temperature phase transition in this material. On the other hand, the quality of the $KIn(MoO_4)_2$ crystals is very high, enabling the effective excitation of Cr^{3+} ions by an argon laser. The similarity of the intensities of the green emission for all the double molybdates studied indicates that this emission is connected to the host type and should be explained in terms of luminescence properties of other scheelite molybdates. Kröger [30] and Blasse and co-workers [31–33] have studied a number of luminescent molybdates of the $M^{II}MoO_4$ type containing molybdate tetrahedra. These compounds show a green emission under optical band-gap excitation. Under excitation into the tail of the band gap, an orange emission was observed. The green band was explained as the intrinsic molybdate emission, whereas the orange emission was due to a defect centre [33]. It is therefore clear that the green emission is connected with the structural properties of the molybdate host corresponding to the spin-forbidden transition from the $^3T_1$ level of the MoO_4^{2-} anion. Another feature which supports this explanation is the similarity of the decay times determined in the present paper and those reported by Blasse for simple molybdates [33].

3.4. ESR studies

ESR investigations have been carried out for powdered or polycrystalline samples at room temperature and 5 K. Among the great number of results obtained from the ESR measurements some representative spectra have been chosen for the most effective Cr^{3+} concentrations. Figure 4 shows the ESR spectra measured at 300 and 5 K for the following molybdate crystals: $LiIn_{0.98}Cr_{0.02}(MoO_4)_2$, $NaIn_{0.99}Cr_{0.01}(MoO_4)_2$, $KIn_{0.995}Cr_{0.005}(MoO_4)_2$, $RbIn_{0.98}Cr_{0.02}(MoO_4)_2$ and $CsIn_{0.98}Cr_{0.02}(MoO_4)_2$.

The recorded spectra appeared to have shapes typical for paramagnetic Cr^{3+}-ion centres observed in the electric crystal field of axial or rhombohedral symmetry. The most intense

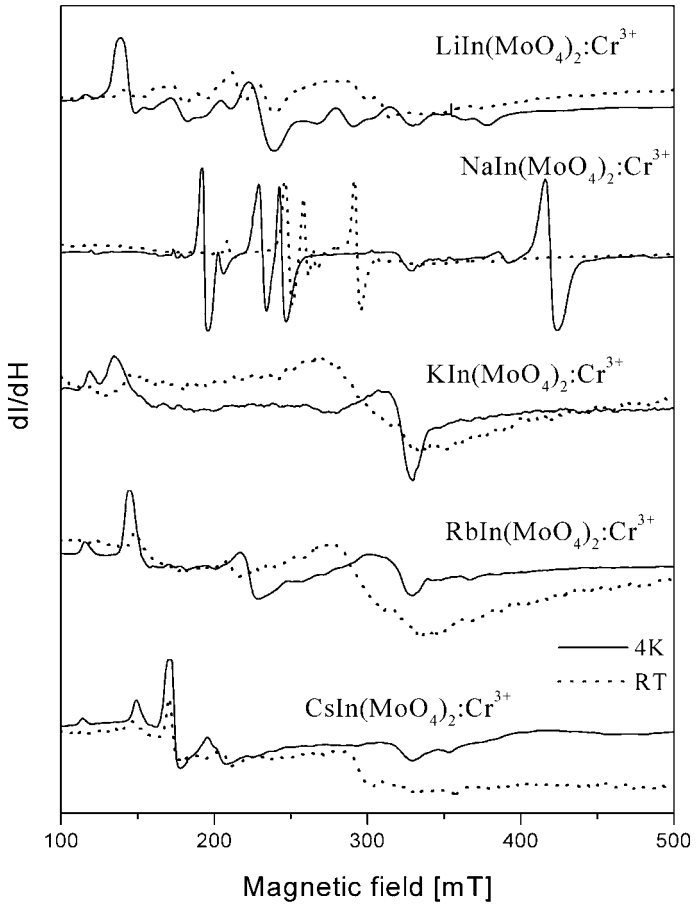

Figure 4. Representative ESR spectra for the most effective concentrations obtained at 5 and 300 K for the crystals studied.

ESR lines appear in the range of low magnetic fields with a resonant field of 130–170 mT. The appearance of the ESR signals of Cr^{3+} ions in the low-magnetic-field range indicates that the so-called zero-field splitting, $2D$, of the $^4A_{2g}$ single orbital state is relatively large in comparison with the energy of the microwave radiation used in the X-band spectrometer. The spectra show the lines arising from the well-known Cr^{3+} centre. These lines reflect very well the number of non-equivalent sites of the active ion and the crystal structure of the double molybdates. Three groups of ESR spectra may be distinguished according to their complexity. To the first group belong the spectra of the molybdates with small numbers of resonant lines, i.e. the spectra of the molybdates with K, Rb and Cs cations. $LiIn(MoO_4)_2$ spectra belong to the second group and the spectra of $NaIn(MoO_4)_2$, which exhibits a very rich ESR pattern, form the third group. This is in agreement with the crystal structure of the molybdate crystals studied. For the orthorhombic K, Rb and Cs molybdates only one type of chromium complex exists, whereas the monoclinic and triclinic structures of $LiIn(MoO_4)_2$ and $NaIn(MoO_4)_2$ have two non-equivalent sites for the trivalent cation. More information about values of spin-Hamiltonian parameters and chromium complexes will be presented in the future, when the studies of the anisotropy of the ESR signals are completed.

The ESR spectra obtained at 5 K do not show any distinct changes when compared to the room temperature results. This applies for all hosts studied. We detected only evidence of the growth of the D-value. Such results suggest that no phase transitions take place in these hosts. From the literature data it is known that $RbIn(MoO_4)_2$ and $CsIn(MoO_4)_2$ crystals may exist at room temperature in two phases: orthorhombic and trigonal. The fact that no changes were observed with decreasing temperature for these hosts proves that the crystals synthesized by us have orthorhombic structure.

4. Conclusions

We have studied the optical properties of Cr^{3+}-doped alkali–indium double molybdates. The active ion enters into at least two crystallographic sites in the sodium derivative and one site in the other crystals studied. Among the systems studied the $KIn_{1-x}Cr_x(MoO_4)_2$ crystal seems to be the most promising laser material. It should be noted that these crystals form a very interesting class of compounds which have the energies of the quartet levels located very low.

Acknowledgment

This work was supported by the Committee for Scientific Research under grant No 3TO9A 057 13.

References

[1] Kuleshov N V, Lagatsky A A, Shcherbitsky V G, Mikhailov V P, Heumann E, Jensen T, Diening A and Huber G 1997 *Appl. Phys.* B **64** 409
[2] Brilingas A, Grigas I, Gurskas A, Zvyagin A I, Kalesinskas V and Pelich L N 1980 *Sov. Phys.–Solid State* **22** 2039
[3] Otko A I, Nesterenko N M and Povstyanyi L V 1978 *Phys. Status Solidi* a **46** 577
[4] Otko A I, Nesterenko N M and Zvyagin A I 1979 *Bull. Acad. Sci. USSR Phys. Ser.* **4** 1675
[5] Nesterenko N M, Fomin V I and Kutko V I 1982 *Sov. J. Low Temp. Phys.* **8** 86
[6] Zapart W 1990 *Phys. Status Solidi* a **118** 447
[7] Zapart M B and Zapart W 1993 *Phase Transitions* **43** 173
[8] Zapart W and Zapart M B 1990 *Phys. Status Solidi* a **121** K43
[9] Hara K, Takenaka H and Ishibashi Y 1988 *J. Phys. Soc. Japan* **57** 3220 and references therein
[10] David W I F and Glazer A M 1979 *Phase Transitions* **1** 155
[11] David W I F 1983 *Mater. Res. Bull.* **18** 749
[12] Kaminskii A A, Li L, Butashin A V, Mironov V S, Pavlyuk A A, Bagayev S N and Ueda K 1997 *Japan. J. Appl. Phys.* II **36** L107
[13] Klevtsov P V, Kozeeva L P and Kharchenko L Yu 1975 *Sov. Phys.–Crystallogr.* **20** 1210
[14] Klevtsova R F and Klevtsov P V 1972 *Sov. Phys.–Crystallogr.* **17** 955
[15] Klevtsova R F and Klevtsov P V 1971 *Sov. Phys.–Crystallogr.* **16** 292
[16] Efremov V A, Trunov V K and Velikodnyi Yu A 1971 *Russ. J. Inorg. Chem.* **16** 1052
[17] Fano U 1961 *Phys. Rev.* **124** 1866
[18] Fano U and Cooper J W 1965 *Phys. Rev.* **137** A1364
[19] Sturge M. D, Guggenheim H J and Pryce M H L 1970 *Phys. Rev.* B **2** 2459
[20] Lempicki A, Andrews L, Nettel S J, McCollum B C and Solomon E I 1980 *Phys. Rev. Lett*. **44** 1234
[21] Hanuza J, Mączka M, Hermanowicz K, Dereń P J, Strek W, Folcik L and Drulis H 1999 *J. Solid State Chem.* **148** 468
[22] Hermanowicz K, Mączka M, Dereń P J, Hanuza J, Strek W and Drulis H 2000 *J. Lumin.* **92** 151
[23] Keil T H 1965 *Phys. Rev.* **140** A601
[24] Henderson B and Imbusch G F 1989 *Optical Spectroscopy of Inorganic Solids* (Oxford: Clarendon)
[25] Mączka M, Hanuza J and Pietraszko A 2000 *J. Solid State Chem.* **152** 498
[26] Mączka M 1997 *J. Solid State Chem.* **129** 287

[27] Mączka M 1999 *J. Raman Spectrosc.* **30** 971
[28] Payne S A, Chase L L, Smith L K, Kway W L and Krupke W F 1992 *IEEE J. Quantum Electron.* **28** 2619
[29] Struck C W and Fonger W H 1979 *J. Lumin.* **18/19** 101
[30] Kröger F A 1948 *Some Aspects of the Luminescence of Solids* (Amsterdam: Elsevier)
[31] Blasse G and van den Heuvel G P M 1974 *J. Lumin.* **9** 74
[32] Groenink J A, Hakfoort C and Blasse G 1979 *Phys. Status Solidi* a **54** 329
[33] Blasse G 1980 *Struct. Bonding* **42** 1